

The renaissance of the Sabatier reaction and its applications on Earth and in space

Charlotte Vogt¹, Matteo Monai¹, Gert Jan Kramer² and Bert M. Weckhuysen^{1*}

The Sabatier reaction (that is, CO₂ methanation) is undergoing a revival for two main reasons. First, the power-to-gas concept offers the prospect of large-scale recycling of (point source) CO₂ emissions, in combination with the use of large quantities of renewable energy to form methane. When this can be achieved in a cost-effective manner, it can use the gas distribution infrastructure that already exists. However, methanation is no simple panacea to the detrimental environmental effect of CO₂ emissions, and reaction products other than methane should also be targeted. Second, methanation has been identified as an important reaction to facilitate long-term space exploration missions by space agencies, such as NASA. This Perspective discusses the current understanding of CO₂ hydrogenation within these concepts, from fundamental mechanistic aspects to several parameters that will ultimately define its technical and economic feasibility on Earth and in space, as we transition into the era of small-molecule activation.

In ‘Nouvelles synthèses du méthane’ (1902), French chemist Paul Sabatier described his findings with regards to the reaction “of the oxides of carbon” in the presence of hydrogen along with finely divided nickel^{1,2}. The combination of these two reactants, a catalyst and elevated temperatures proved to form at least one new molecule: methane³. The discovery of CO₂ methanation (now also known as the Sabatier reaction, which follows equation (1), where ΔH is formation enthalpy) ultimately led Paul Sabatier to become the co-recipient of the Nobel Prize in Chemistry in 1912, alongside Victor Grignard.



Historically, the main industrial application of methanation has been the removal of catalyst-poisoning traces of CO and CO₂ from H₂-rich feed gases in, for example, ammonia plants. Following the oil crisis of the 1970s, CO₂ methanation was studied as an alternative to CO methanation for methane production, in an effort to exploit effluent gases other than syngas. However, only a few concepts reached the commercial scale due to operation hurdles. In the past decade, CO₂ methanation has attracted renewed interest. It is no longer regarded a mere purification step, but rather as a synthetic process with great potential impact for environmental remediation, renewable energy storage and long-term space exploration missions.

In this Perspective, we discuss the scale of global carbon recycling and the role that point sources of CO₂ emissions versus direct air capture (DAC) can play in reaching given targets for global temperature increase. Later, we discuss the feasibility of power-to-methane (PtM) and define boundary conditions for its deployment. In a similar fashion, the role of the Sabatier reaction for long-term extraterrestrial exploration missions is discussed. Finally, recent scientific advances in CO₂ hydrogenation are discussed and pillars for further research are identified, considering its application both on Earth and in space.

Potential applications of the Sabatier reaction

A new era is in its infancy: one that will be defined by pasting small carbon molecules, rather than cutting large ones (for example,

crude oil); one that will be shaped by recycling, electricity and renewable hydrogen. The Sabatier reaction has received much attention recently, and here we identify boundary conditions for its application. Some interesting review papers on this topic have been recently published in the literature^{4–9}.

CO₂ from waste to resource. There are only about five years left until the carbon budget for a 50% chance of staying under 1.5 °C global temperature increase relative to pre-industrial levels is used up (Fig. 1)¹⁰. Society is evidently struggling to respond in a timely manner to this massive challenge^{11,12}. A great deal of current scientific effort is thus being spent to accelerate the energy transition from a fossil fuel-based society to one that is based more on renewable carbon resources¹³. For the physical sciences, the challenge is to make carbon flows circular (that is, to fully retain and recycle carbon flows, in closed-cycle processes). The challenge will require a rather complex scheme involving and incentivizing multiple actors that will heavily rely on sociographically dependent drivers, for example, developed (clusters of) economies with the foresight and capability to financially incentivize carbon-neutral and -negative strategies, along with available point sources of CO₂ that are close to large-scale renewable electricity production. It is important to note that the additional deployment of renewable electricity sources should first be used to phase-out fossil fuel-based electricity production. The role PtM can play in this will be discussed later in the text. Furthermore, it is important to note that scientific discoveries and technological breakthroughs are important pillars of energy transition strategies, but there are other determining factors at play that will be decisive in the ultimate timely halt to global warming. These factors are of a political nature (legislature), as well as sociographic (in this case, for example, societal support) and economic (amortized capital expenditures).

Future energy scenarios. From 2005 to 2014, atmospheric CO₂ levels increased at a rate of 2.11 ppm (roughly 3×10^{14} moles) per year, which is one-third of all energy-related fossil carbon consumption, and coincidentally the same as the world's crude oil carbon

¹Inorganic Chemistry and Catalysis Group, Debye Institute for Nanomaterials Science, Utrecht University, Utrecht, The Netherlands. ²Copernicus Institute of Sustainable Development, Utrecht University, Utrecht, The Netherlands. *e-mail: B.M.Weckhuysen@uu.nl

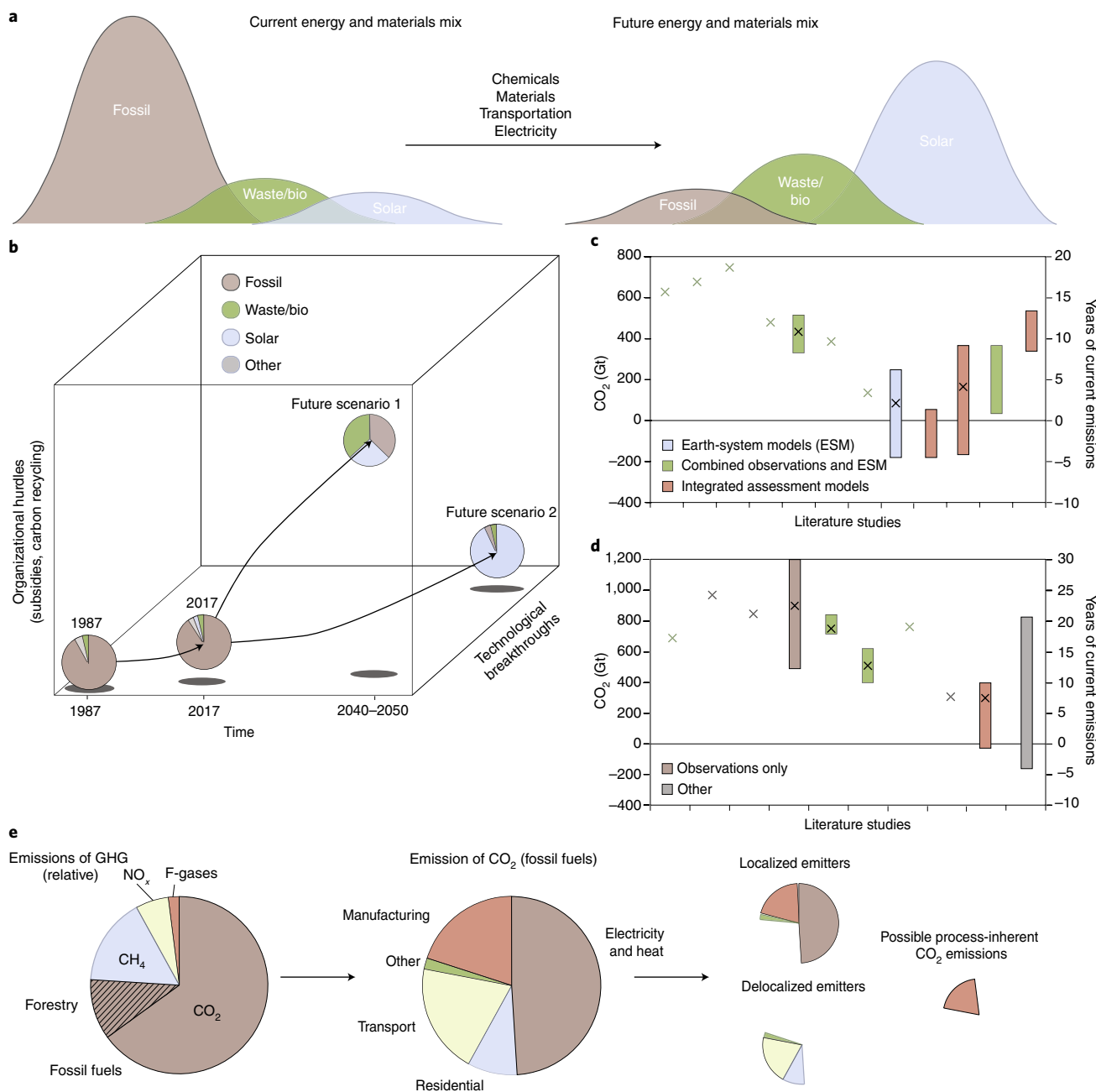


Fig. 1 | Carbon budget and future scenarios. **a**, Schematic showing the transition from a society in 2017 that is largely (~80%) fossil fuel resource-based, to one that employs multiple modes of energy and materials sources. Bio, biomass. **b**, Future energy and materials mix scenarios based on the degree of technological breakthroughs, versus organizational hurdles to be overcome. **c,d**, Remaining carbon budget from various studies, which show the 66% chance (**c**) and 50% chance (**d**) that the global temperature increase will be limited to 1.5 °C above pre-industrial levels¹¹. **e**, Emissions of greenhouse gases (GHG), CO₂ emission sources and separation of sources based on type (localized/delocalized). F gases, fluorinated gases. Panels **c** and **d** adapted from ref. ¹¹, Carbon Brief.

consumption. The carbon content of the 200 ppm increase in CO₂ emissions since the industrial revolution is equivalent to a carbon content of roughly 3×10^{12} barrels of oil, or approximately 90 years' worth of the current annual oil consumption (assuming 6 barrels to a metric ton of oil, and purely CH₂ fractions in it).

The myriad of 50–100 year future energy scenarios that include solar fuels can be grouped into two main possibilities. The first envisages the world to be fully run on renewables, chiefly renewable power, and solar fuels (hydrogen or synthetic hydrocarbons produced from it), to make up for a shortfall of biomass to supply

renewable fuels. Such a future depends on technological breakthroughs, notably for solar fuels. The alternative is a mixed-use scenario in which renewables provide less than full coverage of the energy needs and biomass and fossil fuels continue to be significant parts of the energy mix, coupled with carbon capture and storage^{10,14–16}. Indeed, the energy sector has physical limits to deployment of new technology, as there is a timescale of decades and trillion dollar investments to be made to reach even 1% of the world energy share¹⁷. However, carbon emissions ought to be reduced in 0–15 years to meet the 1.5 °C global warming threshold

(Fig. 1c,d). To curb current emissions, it is important to distinguish between localized (point sources) and delocalized emitters. Localized sources, such as electricity production, industry and heat generation, currently account for roughly 70% of annual CO₂ emissions¹⁸, which can be captured at relatively low cost¹⁹ (Fig. 1e). It is also important to stress here the likely transition of emitting sectors to non-emitters and the timescale thereof. That is, for point sources, electricity generation is likely to be fully displaced by renewables. Some forms of industry, however, are less likely to make this transition. For example, the cement industry currently relies on the conversion of limestone to lime, a process that inevitably emits CO₂, independent of the power sources employed. Moreover, it will take decades before renewables completely take over fossil fuels in the production of electricity and heat, especially in developing countries, so we will be emitting via point sources for decades to come.

Once captured, CO₂ can either be stored (for example, in deep geological formations or by the formation of carbonates) or converted to useful chemical feedstocks/energy carriers using excess carbon-neutral renewable electricity supplies to power the processes (Fig. 2). Carbon capture and storage may help to mitigate CO₂ emissions in the short term; however, it is costly, as approximately 10–40% of the energy of a given power plant is required to capture and store the carbon emissions it thereby produces by fossil fuel consumption²⁰. Carbon capture and storage is a treatment of the symptoms rather than the cause (but is nevertheless likely to be necessary for negative carbon emissions), and is usually met with public opposition (a ‘not in my backyard’ response). Via carbon capture and utilization, rather, the existing resource base can be broadened. In a sustainable carbon cycle strategy, the direct or indirect conversion of CO₂ is envisaged.

The direct conversion of CO₂ to products (rather than, for example, via a syngas production step) limits the feasible synthetic pathways to high-added-value end products, but keeps costs low.

Only in the future (for example, when a large share of the energy supply has been made renewable) should we consider any contribution to lowering CO₂ emissions from DAC (Fig. 2b). Concentrating a stream of 400 ppm CO₂ from delocalized emitters via DAC will inherently be more expensive than capture at point sources. The low technology readiness level of many DAC technologies makes their cost estimates uncertain at this stage^{21–25}. What is clear is that DAC requires technological breakthroughs to become economically viable. Based on the laws of energy-technology deployment¹⁷ it thus cannot have a significant effect on the reduction of CO₂ levels to meet the 1.5 °C global temperature increase target. In the coming decades, the only break-even options for the utilization of current DAC CO₂ technology are high-added-value products that preferentially will not readily be re-emitted into the Earth’s atmosphere, such as (building) materials. However, the feasibility of these options is cancelled out by the fact that high-added-value products will by default be niche (small-scale) applications, while DAC technologies require large-scale deployment. Owing to these uncertainties, technological and legislative breakthroughs will determine whether DAC can play a role in lowering atmospheric CO₂ concentrations; hence likely only after we have successfully employed point-source CO₂ utilization technologies and further emission-prevention strategies (such as, sustainably produced electricity, electrical cars and so on).

The Sabatier reaction in the clean energy transition

Electric grid stability is a major issue in the case of total renewable reliance^{13,26}. Seasonal renewable electricity demand and supply demodulation in Europe is estimated to amount to 480 TWh, or 15% of the total demand, calling for the use of energy buffers/carriers²⁷. Such buffers should be: easily stored and dispatched, that is, integrated with current infrastructures; efficiently converted back to power; economically feasible (environmental policies can have a

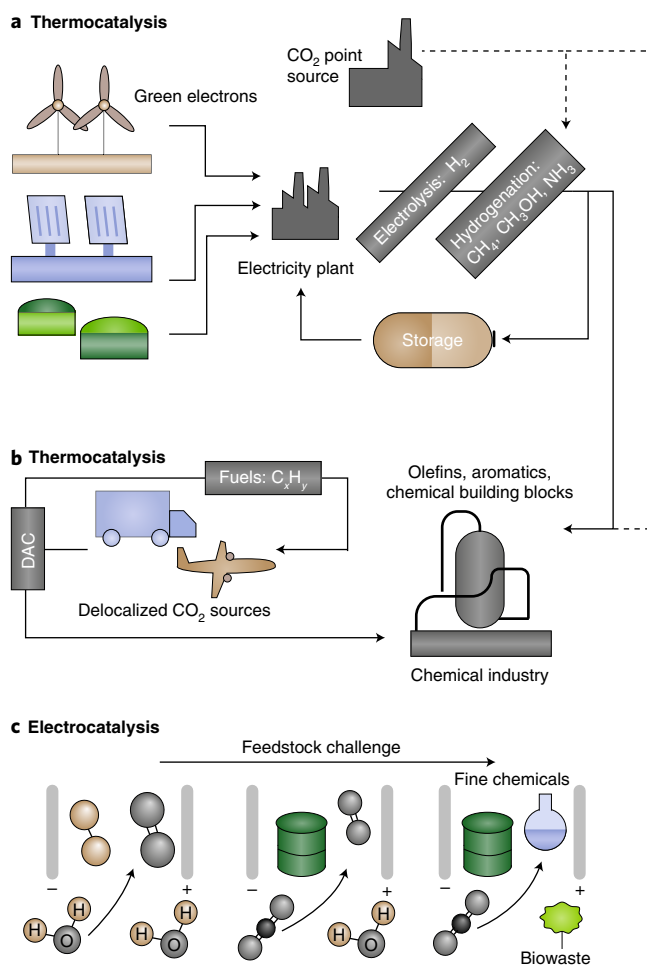


Fig. 2 | Schematic overview of the proposed pathways towards non-fossil-based fuels and chemicals.

a, The high technology readiness level of thermocatalytic-based processes, such as the Sabatier reaction, ensure that this type of technology may be applied to directly reduce point-source emissions of CO₂, and aid in the storage of electricity via chemical bonds. **b**, The next challenge in heterogeneous catalysis is to make value-added chemicals from CO₂ emissions, and to bring down the costs of DAC. **c**, Electrocatalysis is likely to play a much larger role in the production of chemicals and fuels in the future. These technologies, however, require a lot of research effort, and will thus only play a role in the more distant future. The feedstock challenge in electrocatalysis is indicated from left to right: first, to bring down the cost of electrolysers splitting water into hydrogen; second, to use CO₂ and water to produce value-added chemicals (CO₂ to higher hydrocarbons); and third, the most advanced mode of operation, in which green electrons are used to valorize biomass (for example, oxidizing lignin- and (hemi-)cellulose-derived chemical building blocks), and at the same time reduce CO₂ to more valuable chemicals. Panels adapted from: **a,b**, ref. ³⁹, Springer Nature Ltd.

big impact); and, finally, safe, sustainable and accepted by the public. Table 1 summarizes important advantages and disadvantages of several different power-to-X (PtX) technologies.

CO₂-to-methane technologies meet many of these requirements; however, the main drawback is that they are not economically competitive with natural gas or other substitute natural gas (SNG) sources, mainly due to the cost of the electrolysis step²⁸. Since the production of electricity from methane requires a two hour start-up time, PtM would indeed only be suitable for long-term electricity storage²⁹.

Table 1 | Advantages and disadvantages of different power-to-X processes for storing green electrons

Process (power-to-X)	Advantages	Disadvantages	Green electrons needed	Density (kg m ⁻³)	Specific energy (MJ kg ⁻¹) ^a	Energy density (MJ m ⁻³) ^a
Hydrogen	<ul style="list-style-type: none"> • Suitable for offshore production 	<ul style="list-style-type: none"> • Gas (lower energy density) • Corrosive and explosive • Expensive storage and distribution 	2	0.090 ^b	141.7	12.7
Methane (liquefied natural gas) ^c	<ul style="list-style-type: none"> • Point-source CO₂ abatement • Infrastructure available • High-energy-density gas 	<ul style="list-style-type: none"> • Gas • Lowest market value product • Not suitable for offshore production and storage of electricity (point-source CO₂ required) 	8 (-8)	0.716 ^b (428)	55.5 (55.2)	39.8 (23,625)
Ammonia	<ul style="list-style-type: none"> • Transported as water solution or anhydrous (high density) • Mobility of production (N₂ to be captured everywhere) 	<ul style="list-style-type: none"> • Safety, yet much industrial experience 	3	352 ^d	22.5	7,920
Methanol	<ul style="list-style-type: none"> • Liquid • Easy storage/distribution • High market value product • Point-source CO₂ abatement 	<ul style="list-style-type: none"> • Not suitable for offshore production and storage of electricity (point-source CO₂ required) 	6	791	23.0	18,200
Kerosene (C ₁₀ -C ₁₆)	<ul style="list-style-type: none"> • Wax, jet fuel • Easy storage/distribution • Highest market value product • Point-source CO₂ abatement 	<ul style="list-style-type: none"> • Not suitable for offshore production and storage of electricity (point-source CO₂ required) • No direct catalytic conversion from CO₂^f 	6.2-6.13 ^e	821	43.0	35,300

^aHigher heating value (the water of combustion is entirely condensed and the heat contained in the water vapour is recovered). ^bAt standard temperature and pressure. ^cWorld trade already in place, but requires cooling to -162 °C. ^dAssuming transportation as water solution⁶⁴. ^eAverage per carbon atom. ^fCO₂ converted to CO, in turn converted to hydrocarbons via Fischer-Tropsch synthesis⁶⁵.

While hydrogen itself is a decent energy carrier and requires no additional steps after electrolysis, storage is costly. More specifically, storage per weight unit is roughly ten times more expensive than for methane³⁰. Solid and liquid carriers, such as metal hydrides and liquid organic hydrides, are being investigated as ways to store and transport hydrogen, but problems related to technology readiness, storage reversibility and distributed facilities still limit their applicability^{31,32}. Based on these premises, the leveled costs of electricity production, including storage for hydrogen- and methane-based electricity storage scenarios, range from €339 to 632 MWh⁻¹ and from €194 to 1,032 MWh⁻¹, respectively, depending on the full load hours for the methane-based production facility. These relatively high prices would need to be countered by periods of lower electricity cost, for example, with abundant sun/wind, and can only be competitive when the price of fossil fuels or CO₂ emissions are (artificially) high. Without drawing excess value from the exact costs calculated, this exercise shows that there is an economic case to be made for PtM versus power-to-hydrogen when long-term storage (seasonal) of electricity is taken into account. Furthermore, PtM requires the close proximity of renewable electricity (or hydrogen) to point sources of CO₂.

Current CO₂ emissions in Europe amount to 1.3×10^{14} moles yr⁻¹, which, if all converted to methane, can provide 120 TWh of electricity on combustion at 100% efficiency, but only 40 TWh of electricity at a more realistic 34% overall process efficiency. This is an order of magnitude too small to accommodate European seasonal storage requirements. However, under the assumption that this CO₂ will be recycled in a closed-cycle process, the storage capacity could accumulate with the development of the renewable electricity capacity and further phasing-out of CO₂ emitters. The 28 member states of the European Union currently possess 1,214 TWh

of underground natural gas storage capacity (<https://www.gie.eu/>), including pipelines and salt caverns, which confirms the feasibility of PtM for seasonal grid stabilization.

A sometimes-underestimated drawback related to the use of natural gas is that methane is a much more powerful greenhouse gas than CO₂, so that the on-paper benefits of carbon cycling implementation can be outweighed by methane emissions along the natural gas value chain. To address this problem, new guiding principles are currently being adopted by major natural gas companies, aimed at controlling and reducing methane emissions by modernization of the existing infrastructure (<https://tyndp.entsoe.eu/tyndp2018/power-system-2040/>). The production of methane from CO₂ can only result in net-neutral carbon emissions in a closed-cycle process and by making use of non-fossil-fuel-based electricity, as illustrated in Fig. 2a. Yet we should note that the benefits of scaling-up renewable electricity to phase-out coal and other fossil fuel-based power plants should have priority over the renewable production of methane. Thus, the feasibility of the power-to-gas concept has a sweet spot with respect to time — that is, when the share of renewable electricity is large enough to require green storage processes but there are still enough CO₂-emitting processes — and geographical location, due to the requirement for the production of green electrons to be located with point sources of CO₂. An illustrative example of what may prove to be a feasible concept is the cooperation of the iron or cement industries with the energy sector to provide enough CO₂ emissions, which they can use to seasonally store electricity, recycling burned methane. For economic viability, some time is still needed for the development of cheaper electrolysis, and phasing-out of more fossil fuel-based electricity (Fig. 2a). Furthermore, it is noteworthy that without adequate adoption of delocalized carbon capture legislation and facilities, delocalizing CO₂ point sources via

the redistribution of PtM-produced methane into the natural gas network may even harm the feasibility of the previous example (as a very large fraction of localized CO₂ emissions are needed for the seasonal storage of electricity).

It must be further noted that the feasibility of this concept, and most CO₂ emission-reducing concepts with significant impact, rely on a legislative push away from fossil fuels, via either carbon or fossil fuels taxation. The implementation of a carbon tax will further be a positive reinforcement for the use of methane as a main fuel as we move away from coal, and later from oil, as the CO₂ emitted per unit of energy produced is lower.

Furthermore, improvements should be made to reactor designs to accommodate the highly exothermic CO₂ hydrogenation reaction, such as a three-phase reactor allowing for increased applicability of PtM in intermittent or dynamic operation, an important parameter in the feasibility of the power-to-gas concept²⁸.

CO₂ methanation in practice. As far as we are aware, the so-called e-gas plant in Werlte, Germany, commissioned in 2013, is the biggest commercial CO₂ methanation plant worldwide. A few other examples of operational PtM facilities exist or are currently under construction, mainly at the pilot scale³³. The Werlte plant produces methane starting from CO₂ captured from biogas produced close by via amine scrubbing, and from H₂ generated by three KOH-based alkaline electrolyzers powered by wind energy with a total capacity of 6 MW. It was qualified in 2015 to participate in the electric grid market³⁴. The plant can be up and running in five minutes, to balance out even slight load changes in the electricity grid. The hydrogen produced from the electrolysis is filtered to eliminate KOH aerosols, and dehydrated and compressed to 10 bar for storage in a buffer tank worth one hour of methanator operation. This allows for a decoupling of operation between the electrolyser and the methanator units. The methanator consists of a long bundle of tube reactors, loaded with a nickel-based catalyst. The produced methane is dried and fed into the natural gas grid. Water is cycled back in the electrolyzers, while oxygen produced at the anode of the electrolyser is vented out. The methanation reactor is cooled by molten salts and the heat is used to regenerate the amine scrubber, bringing the process efficiency to ~72% (ref. ²⁸).

The Sabatier reaction in space. At present, the Sabatier reaction is mainly used in space exploration as a means to produce water, and methane is vented³⁵. However, improving the PtM process for, for example, reusable launch systems, is vital for long-term manned missions, such as those to Mars. Related to this, the rocket propellants Hydralox (hydrogen and liquid oxygen (LOX)) and RP-1 (kerosene and LOX) are being phased-out by liquid methane and LOX for multiple reasons. Compared with hydrogen, methane is more stable in space, as it does not cause metal embrittlement, has a boiling point similar to that of oxygen (enabling simpler bulkhead design) and does not need bulky highly insulated cryogenic tanks³⁶. Compared with kerosene, methane is lighter, burns at higher temperature and does not cause coking, with the only disadvantage being its lower energy density (bigger tanks required). Most importantly, methane can be manufactured from CO₂ by the Sabatier process, making it appealing for long-term space exploration (for example, trips to Mars).

In 2011, a Sabatier reaction system was integrated into the International Space Station water recovery system, and a prototype of a Mars in situ propellant production system was demonstrated, using CO₂ from a simulated Mars atmosphere (which contains 96% CO₂) and H₂ from propellant to produce a mass leverage of 18:1 in useful rocket propellant produced on Mars compared with imported feedstock^{35,36}. On Mars, methane is to be recycled in a similar way via the in situ resource utilization approach. Here, exhaled CO₂ or CO₂ from Mars' atmosphere can be combined with hydrogen,

which is a byproduct of electrolysis of water (mined on Mars) for O₂ production for the astronauts to breathe. Durability in these systems is more important than costs, which results in catalysts such as ruthenium being the metal of choice.

As recommended by NASA for the employment of the Sabatier reaction for Mars exploration, research efforts should be directed in the employment of catalyst systems that are directly compatible with Mars' atmosphere (CO₂, N₂, Ar)³⁶. In this respect, water vapour permselective membranes should be developed to enhance the activity of the catalyst according to Le Chatelier's principle, separating water streams to be recycled for life support or in the electrolysis step. As a side note, NASA recommends the industry stimulation for the development of electrolyzers (that may also be used for extraterrestrial space exploration). Electrolysis of CO₂ in ionic liquids and the electrocatalytic reduction of CO₂ and H₂O to CH₄ and O₂ show great potential, but have a lower technology readiness level than, for example, traditional heterogeneous catalysis³⁶.

Fundamentals of the Sabatier reaction

Supported nickel catalysts are generally considered to be excellent methanation catalysts, due to their ability to split CO bonds and their relatively high hydrogenation activity³⁷. Furthermore, nickel catalysts are cost-effective alternatives to other highly active, noble metal hydrogenation catalysts (for example, ruthenium and rhodium)⁵. Nevertheless at temperatures <300 °C, nickel is prone to deactivation via oxidation and, of higher concern, to highly toxic Ni(CO)₄ formation³⁸.

A wide variety of spectroscopic and theoretical studies have been carried out, and, on the basis of these studies, we are able to discern with great probability active pathways for CO₂ hydrogenation over nickel.

Proposed mechanisms for the Sabatier reaction. Recent advances have been made to unravel the mechanism of the Sabatier reaction^{39–41}. There are three conceivable pathways towards methane synthesis (Fig. 3). The first is the carbide pathway, in which CO₂ dissociates to form CO. It is commonly agreed on in the literature that for Ni/SiO₂ catalysts, the carbide pathway is the main active pathway^{5,42}. The second plausible pathway is the formate pathway, the existence of which has been proven by operando spectroscopic techniques (mainly Fourier transform infrared spectroscopy), but it is deemed inactive for SiO₂-supported nickel catalysts^{39–41}. Third is a carboxyl pathway. Intermediates from this pathway have not been reported in the literature and none of the intermediates or products expected from it (for example, methanol) have been reported in literature; thus we regard this pathway as inactive on Ni/SiO₂ catalysts.

Interplay between pathways, mainly the carbide and the formate pathways, via, for example, H-assisted CO dissociation, is reasonable for CO₂ methanation as the energy barrier for direct CO dissociation is relatively high. It is important to stress here also that the reducibility of the support of the catalysts can play a big role in the delocalization of electrons around adsorbed CO or CO₂, which can effectively increase the facility of such a step, ultimately leading to higher activity.

Drawing similarities between CO₂ methanation and CO oxidation/reduction, and methanol synthesis yields important mechanistic insights to tune the selectivity of each of these reactions and builds the ground for the integration of knowledge across a wider span of chemical reactions^{43–47}. For example, extensive literature on CO methanation shows that the rate-determining step is the H-assisted CO dissociation⁴⁸, which holds for CO₂ methanation as well^{9,39}. The choice of metal affects the inherent rate of hydrogenation, as well as CO dissociation and the eventual selectivity of CO₂ towards methane or C–C coupled fragments. A catalyst with (reverse) water–gas shift ((R)WGS) activity, CO dissociation capability and the ability

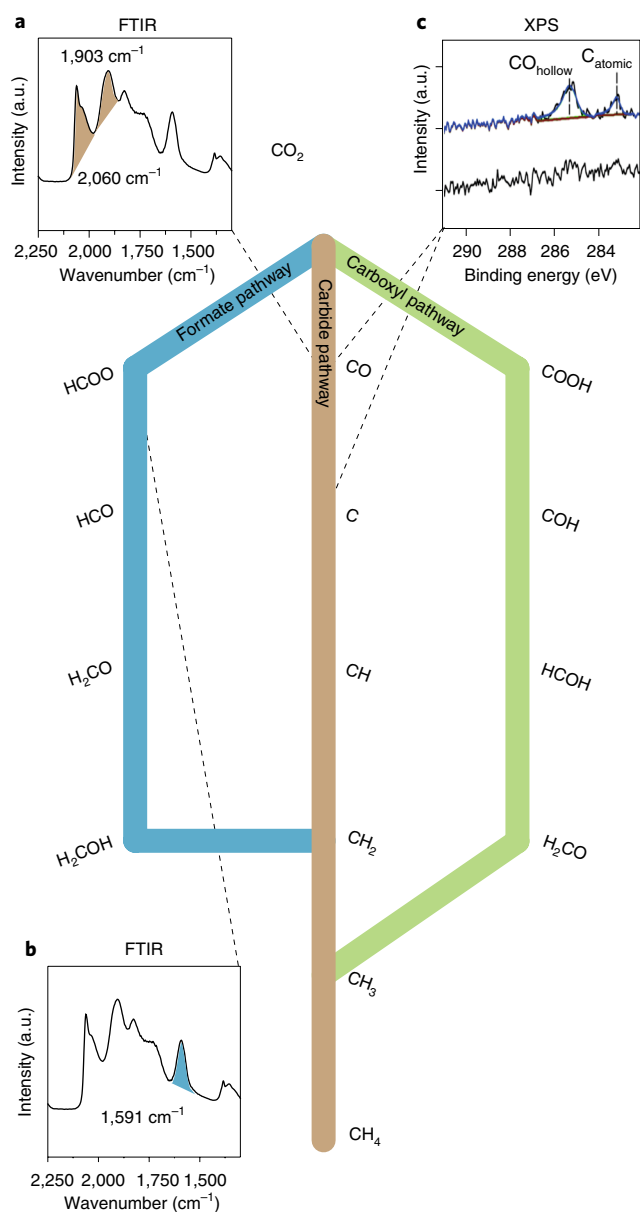


Fig. 3 | Possible reaction pathways for the methanation of CO₂.

a, Operando Fourier transform infrared spectroscopy (FTIR) confirmed the presence of gaseous CO, adsorbed CO in the bridge (inactive) and top (active) positions on SiO₂-supported Ni nanoparticles^{39,86,87}. **b**, Operando FTIR confirmed the presence of formate species on SiO₂-supported Ni nanoparticles^{39,87}. **c**, In-situ ambient-pressure X-ray photoemission spectroscopy (XPS) detected the presence of surface CO and C species on Ni(111)⁴⁰. Black, 20 mTorr CO₂ + 200 mTorr H₂; blue, 100 mTorr CO₂ + 200 mTorr H₂. Panel **c** adapted from ref. [40], American Chemical Society.

to dissociate H should — in theory — be able to produce C₂₊ fragments from CO₂. Cobalt, iron and also the often-neglected nickel are capable of doing so. However, RWGS thermodynamics and that of increased hydrocarbon chain growth are inversely related, which leads to low yields and overall limited success for the direct hydrogenation of CO₂ to C₂₊ hydrocarbons via heterogeneous catalysis⁷. Understanding the mechanism can also help to avoid CO₂ methanation in selected technologies. For example, recent advances have been made in selective CO methanation, inhibiting the methanation of CO₂ on Ni/CeO₂, which is interesting for proton exchange membrane fuel cells applications^{49,50}.

Tuning CO₂ reduction via structure sensitivity, metals and promoters. Figure 4 summarizes the literature on CO₂ reduction, in the gas phase (thermocatalysis, Fig. 4a) and in the liquid phase (electrocatalysis, Fig. 4b). It is noted that both base and noble metals are active. For gas-phase CO₂ hydrogenation, there is a gradual increase in the turnover frequencies (TOFs) with increasing reaction temperature. Furthermore, whereas Ni, Ru and Rh mainly produce CH₄, Cu produces CH₃OH, while Pt makes only CO. Fe, Co and Ir produce mixtures of CO and CH₄. In the case of liquid-phase CO₂ reduction, TOFs increase with increasing voltage. Most base and noble metals produce CO as the main reaction product; however, Cu turns out to be a very versatile electrocatalyst, as formate, methane and ethylene can be made. Comparing Fig. 4a with Fig. 4b, one notices that the TOF values are generally an order of magnitude higher for electrocatalysis than for thermocatalysis. To realize the potential electrocatalysis has for high-density throughput, however, advances in process engineering are still required.

CO₂ reduction is also a structure-sensitive reaction, as noted for Ni, Co, Cu and Pd in Fig. 4c (thermocatalysis) and for Pd in Fig. 4d (electrocatalysis)³⁹. That is, the TOF varies with metal particle size in supported metal catalysts as not all atoms on a nanoparticle surface have the same activity^{39,51}. In other words, one can tune the overall reactivity of the catalyst by altering the metal particle size. The nomenclature on structure sensitivity has formed around active site configuration, due to the strong focus on surface science in recent decades⁴⁸. However, the growing control over the synthesis of catalytically relevant model systems in recent literature allows us to propose here four main pillars of structure sensitivity (Fig. 5)^{39,52}: active site geometry^{40,53}, degree of atomic behaviour or metal properties of a nanoparticle^{54,55}, dynamic restructuring onset by catalysis or catalytic conditions⁵⁶, and support effects, which can vary in degree of relevance with changing metal particle size⁵⁷. CO₂ reduction is influenced by each of these factors, as can be seen in Fig. 4. Metal-support interactions, in combination with particle size and metal nuclearity, are thus an interesting way to tune the selectivity and activity of CO₂ reduction. This is illustrated in Fig. 5.

An interesting example is a study on Au for the electrocatalytic conversion of CO₂ to CO (ref. 53). Au nanowires possess excellent activities due to their high mass density of reactive edge sites, which show weak CO binding. By making use of different model catalyst systems (that is, nanowires versus nanoparticles), the relative ratio of edge sites to corner sites was changed; hence, the Faraday efficiency could be enhanced (Fig. 5e). In another study, it was demonstrated that atomically dispersed Ni(I) is an active site for the electrochemical reduction of CO₂ into CO (Fig. 5f)⁵⁵. These single Ni^I atoms were made by dispersing them onto a nitrogenated graphene support material. In addition, for the thermocatalytic CO₂ reduction, the metal/support interface can be used to tune the activity and selectivity^{58,59}. For example, a recent study showed how Cu metal nanoparticles supported on SiO₂ and ZrO₂ results in different formation rates of methanol (Fig. 5g)⁵⁸. By using kinetics and various spectroscopies, it was possible to elucidate the origin of the increased methanol formation rate for Cu/ZrO₂. It was found that formate is an intermediate and that the Cu/ZrO₂ interface is key for the conversion of this intermediate to methanol. In another study, catalyst selectivity was tuned by changing the oxide support for PtCo particles (Fig. 5h)⁵⁹. Replacing a TiO₂ support oxide by CeO₂ or ZrO₂ selectively strengthens the binding of CO- and O-bound species at the PtCo-oxide interface, leading to different product selectivity.

To generalize, the inherent reactivity of the CO- and O-bound intermediates at different metal/support interfaces make reducible metal oxides excellent tools for tuning the selectivity of CO₂ reduction^{9,59–62}. CeO₂ in particular shows very interesting properties^{61,63}, and has even been shown to facilitate C–C coupling in low quantities (C.V. et al. manuscript in preparation).

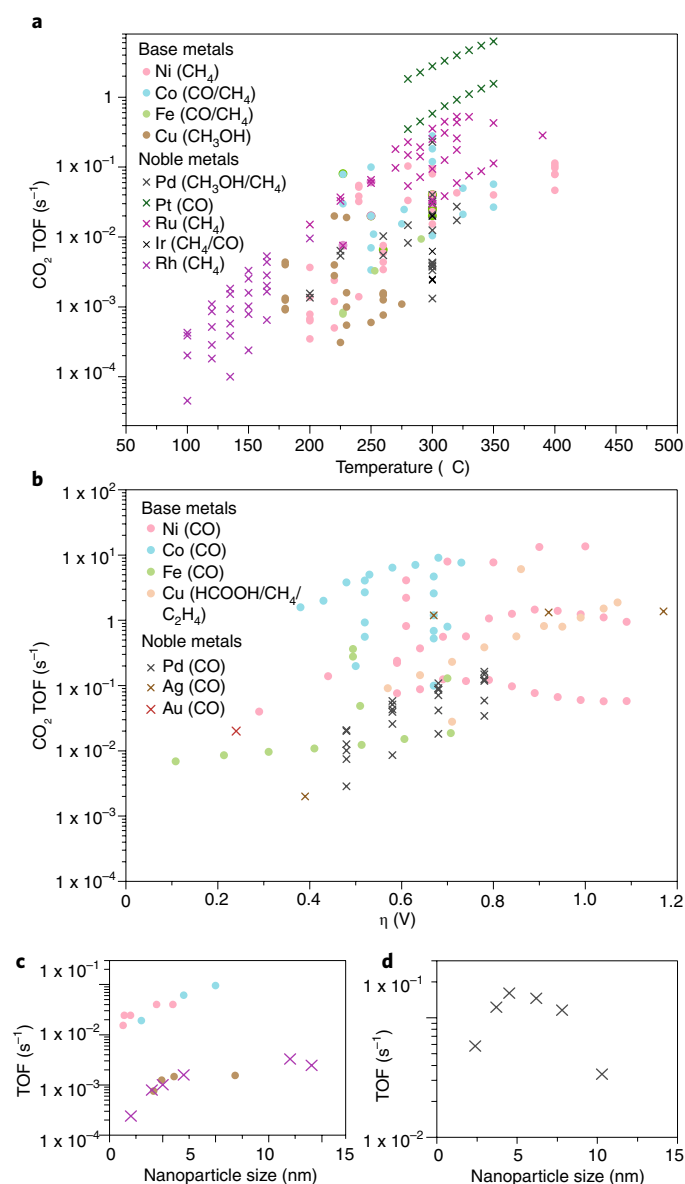


Fig. 4 | An overview of TOF trends found in the literature for thermocatalytic and electrocatalytic CO_2 reduction. **a, b**, TOF versus temperature, as found in literature for various metals and end products for thermocatalysis (**a**) and electrocatalysis (**b**). **c**, Particle size trends found in the literature for heterogeneous catalytic CO_2 hydrogenation over Ni, Co, Cu and Pd. Where η is the overpotential: the difference of the applied potential and the theoretical E_0 for CO_2 electroreduction under the reaction conditions used. **d**, Particle size trends in electrocatalytic CO_2 reduction over Pd. A table listing some experimental parameters and the TOF values with corresponding literature can be found in the Supplementary Information.

Aside from structural enhancement in supported monometallic catalysts, promoters in the form of metallic decoration or alloying allow tuning of selectivity and activity in CO_2 reduction not only towards methane, but also towards value-added reaction products. Here, computational screening (using, for example, machine learning and experimental input) of metal combinations can allow the selection of combinations of materials to bridge the gap between the thermodynamic limitations of well-known catalysts for CO and CO_2 conversion and their operational temperature of the RWGS reaction, and, for example, chain growth.

An excellent example for a promoter in CO_2 methanation is the promotion of Ni with Fe, yielding higher activity and stability in the reaction than either metal alone⁶⁴, as also predicted by computational screening for CO methanation^{65,66}. Nevertheless, there is also still a need for definitive in situ structural evidence of the mechanism of change to the active site, as well as the control of size and composition of the promoted supported metal nanoparticles.

Furthermore, alkali metals are an interesting class of promoters in the PtM concept as the hydrogen evolution reaction often takes place in alkaline solutions. Sodium and potassium have both proved to promote the RWGS reaction, which in turn is an important step in CO_2 methanation^{67–69}.

Liquid-phase versus gas-phase CO_2 methanation. Classical thermocatalytic CO_2 reduction is a two-phase system, where the solid catalyst interacts with gaseous CO_2 and H_2 at elevated temperatures (and pressures) generally in an adiabatic fixed bed reactor⁷⁰. Alternatively, CO_2 methanation can take place in the liquid phase via, for example, biocatalytic conversion of CO_2 . This takes place at milder reaction temperatures of 40–70 °C, and with microorganisms that generally have higher tolerance for the impurities that are found in flue gas streams than conventional heterogeneous catalytic conversion. The biggest challenge in the biocatalytic conversion of CO_2 to methane is arguably the poor solubility of hydrogen in the aqueous phase, which thus becomes a limiting factor in catalytic turnover²⁸. Furthermore, relatively costly mediators or electron equivalents are required as often electrons cannot be directly injected into biocatalysts⁷¹. Biocatalytic routes are at an earlier stage of technology readiness than classical heterogeneous catalytic reactions, which are commercially operative.

CO_2 can also be reduced to methane electrocatalytically. This is particularly interesting as the additional electrolysis step to form hydrogen might be surpassed in this approach, which may have significant overall process efficiency benefits²⁸. However, non-scarce base metals with activity for the electrocatalytic reduction of CO_2 (such as Cu and Ni) are generally also active for the hydrogen evolution reaction⁷². Furthermore, the question is what reaction product is targeted, and it is evident from Fig. 4b that CO is still the main reaction product. Here, the efficient use of green electrons is thus a challenge. For this reason, alternatives to aqueous media are sought, and ionic liquids are an example through which overpotentials can be lowered and Faradaic efficiencies can be improved⁷³. Another interesting approach includes the bioelectrocatalytic reduction of CO_2 , which requires no costly co-factors, combines the two liquid-phase processes and has been successful on a laboratory scale⁷⁴. These alternatives, of course, still need to be able to supply sufficient protons for CO_2 reduction to proceed at desired TOFs.

Thus, adhering to the laws of energy deployment, it is not likely that (bio)(electro)catalytic reduction of CO_2 into methane will be viable at the time and scale of the operational boundary conditions we have here identified for the PtM process. These routes should be considered and further developed on a longer timescale (Fig. 2) for other value chemicals, such as methanol, formate or CO (Table 1).

Integrating electrochemistry in biorefineries. Another route to be followed is to use renewable electricity to perform electrosynthesis reactions on biomass-derived oxygenates. The principle of the genesis of biomass-based chemicals aided by electrocatalysis is presented in Fig. 2c. One route is to lower the oxygen content of biomass-based chemicals^{75,76}. In particular cases, the carbon chain length can be increased in the required range of liquid fuels (for example, kerosene, Table 1). Hence, biomass-derived electrofuels could be made that are in principle fully compatible with the combustion engines of our current transportation fleet. However, it would be advantageous if more valuable oxygenates could be made from, for example, lignin- and (hemi-)cellulose-derived building blocks^{77,78}. In this

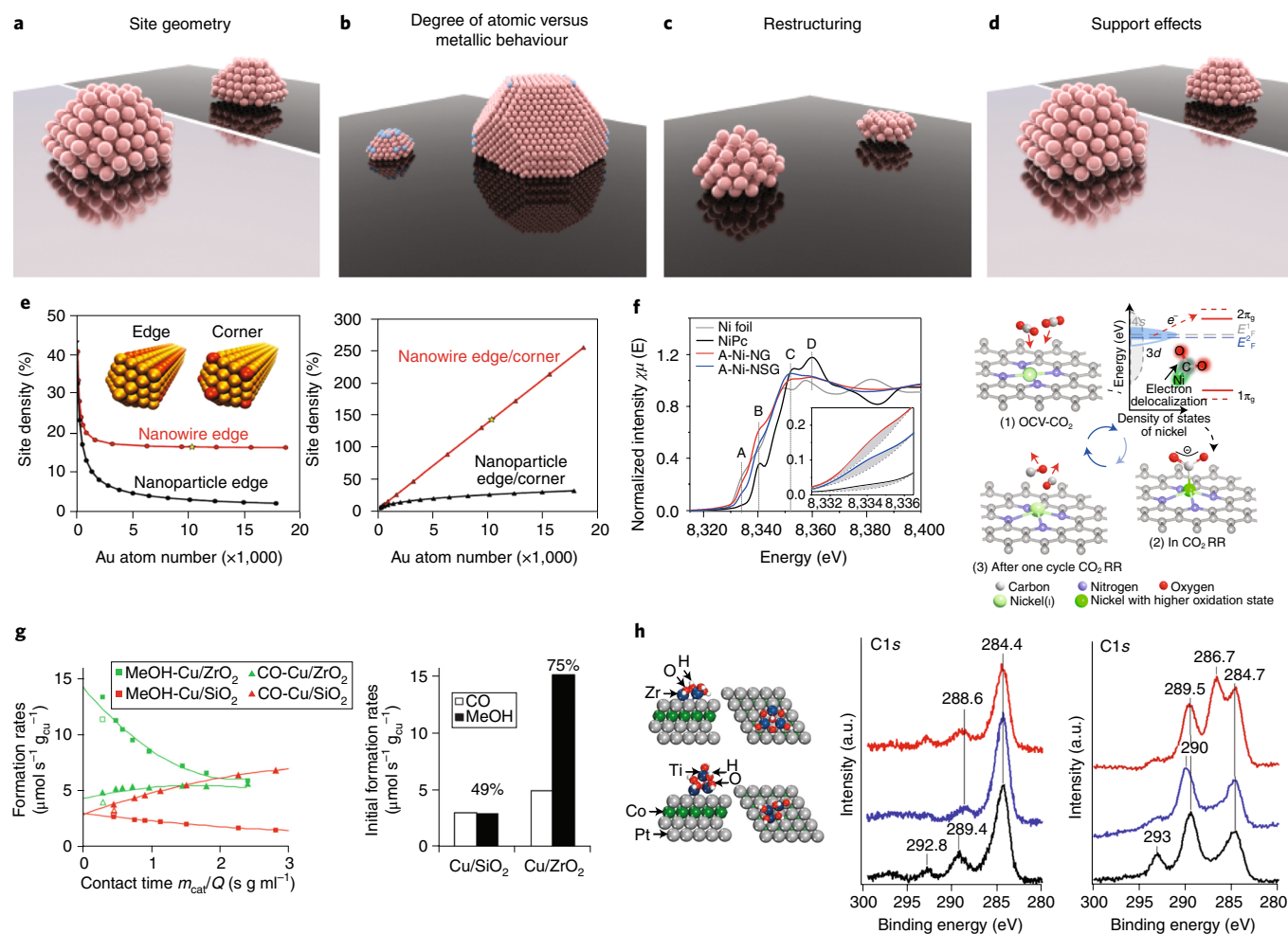


Fig. 5 | Structure sensitivity in thermocatalytic and electrochemical CO $_2$ reduction. **a–d**, Schematic of the importance of site geometry (**a**), the degree of atomic versus metallic behaviour (**b**), restructuring in catalysis (**c**) and support effects (**d**). **e–h**, A literature example for each of the four pillars of structure sensitivity. **e**, A catalyst model for electrochemical CO $_2$ reduction. Left: edge site weight percentage for a 2-nm-wide Au nanowire and an Au nanoparticle as a function of the number of Au atoms. Right: idealized ratios of edge/corner for the Au nanowire and Au nanoparticle⁵³. **f**, Activation processes for CO $_2$ molecules on an atomic Ni site for electrochemical CO $_2$ reduction⁵⁵. NG and NSG are single nickel atom catalysts prepared without and with a sulfur precursor, respectively. Peak A represents 1s to 3d transition, peak B represents 1s to 4p $_z$ transition, C and D represent 1s to 4p $_{x,y}$ transitions and multiple scattering processes, respectively. OCV, open circuit voltage; RR, reduction; A-Ni, atomically dispersed nickel. **g**, The metal/support interface can be used to tune methanol synthesis via thermocatalytic CO $_2$ reduction over Cu⁵⁸. **h**, C1s AP-XPS of PtCo/TiO $_2$ and PtCo/CeO $_2$ after exposure to CO $_2$ (100 mTorr) and H $_2$ (600 mTorr), at 30 °C (black), 250 °C (blue) and subsequent cooling to 30 °C (red). For supported PtCo particles, the selectivity in thermocatalytic CO $_2$ reduction is influenced by the reducibility of the support oxides, for example, TiO $_2$ and ZrO $_2$ (ref. ⁵⁹). Panels adapted from: **e**, ref. ⁵³, American Chemical Society; **f**, ref. ⁵⁵, Springer Nature Ltd; **g**, ref. ⁵⁸, Wiley; **h**, ref. ⁵⁹, Wiley.

manner, bulk as well as fine chemicals could be produced together with CO $_2$ electroreduction, provided (1) we could obtain more fundamental insight in how to tune the selectivity of electrosynthesis and (2) the intrinsic requirements are fulfilled for simultaneously performing both types of reaction at the cathode and anode. This field of research is clearly still in its infancy.

Carbon–carbon coupling. The Sabatier reaction can also offer clues towards the ultimate valorization of CO $_2$ by direct C–C coupling. Control over C–C versus C–H bond formation is key regardless of the final desired product. Much attention is given to the direct conversion of CO $_2$ to C–C coupled fragments, to avoid high capital costs from the two-step RWGS and Fischer–Tropsch synthesis conversion. However, an inherent constraint is that the RWGS equilibrium lies at much higher temperature than hydrocarbon

chain growth probability α for classical Fischer–Tropsch synthesis-type catalysts⁷.

The direct catalytic conversion of CO $_2$ into high-value chemicals has low technology readiness levels. Electrocatalytic conversion of CO $_2$ to ethylene (6e $^-$ /C)⁷⁹ and ethanol (4e $^-$ /C)⁸⁰ has recently been reported, while aromatics (3e $^-$ /C for benzene) have been, for example, produced in one step over a composite catalyst, coupling methanol catalysts with zeolites active for the methanol-to-aromatics reaction⁸¹. Aqueous phase CO $_2$ hydrogenation over Pd–Cu catalysts also resulted in ethanol production at low temperature⁸². Clearly, more research should be directed towards the selective formation of high-value chemicals with multiple C–C bonds.

Catalyst deactivation. A downside of the more traditional nickel-based methanation catalysts is their rapid deactivation at low

temperatures (<250 °C), at which mobile sub-carbonyls are formed^{66,70}. At these low temperatures, noble metals, such as Pt, Ru and Pd, exhibit better stability, yielding interesting model systems, for example, to understand mechanistic details. Recent work has proven that the formation of nickel carbonyls (and thus the deactivation through this mechanism) is also structure sensitive³⁹, though it has already been shown in the literature that particles of 3–4 nm are less stable due to Ni(CO)₄ formation than, for example, 8 nm Ni particles³⁸. Furthermore, it is important to further improve the stability of nickel with respect to sulfurous compounds as a common flue gas contaminant. Here, metal alloying, in combination with the proper support oxide, may be an interesting route, which should be further explored.

Summary and outlook

DAC will not effectively contribute to decreasing CO₂ emissions to meet the 1.5 °C global temperature increase target. While the emissions of point sources of CO₂ should be captured and stored or utilized as fast as possible, the power-to-chemicals principle still awaits its sweet spot for application in many countries with respect to time. A critical mass in the application of renewable electricity should be reached, which requires long-term storage of renewable electricity. Nevertheless, with an abundance of green electrons together with significant point-source CO₂ emissions, PtM could be a viable option for seasonal storage of electricity versus power-to-hydrogen.

For this generation of scientists, the challenge with one of the biggest societal impacts is to bring down the cost of electrolyzers. Within the resulting hydrogen economy, the authors would like to stress that the (economically feasible) conversion of CO₂ to value-added chemicals should be possible with advances in (electro) catalysis. Tuning of heterogeneous catalysis should be attempted via structure sensitivity, supports and promoters based on Fe and Ni to optimize the RWGS activity at lower temperatures and consequently facilitate hydrocarbon chain growth. Similarly, for electrocatalysts, controlling the selectivity of the CO₂ reduction reaction as well as reducing the overpotential for the formation of end products (such as methane or ethylene) are major scientific challenges.

Such advances can only be made when appropriate analysis techniques are (further) developed. To recrudescence the namesake of the reaction discussed in this Perspective, Sabatier was indeed not the first to practically discover hydrogenation reactions but the first to be able to analyse that benzene had converted into cyclohexane (which is currently also a proposed option for chemical hydrogen storage) and demonstrate the conversion of CO₂ into CH₄ (refs. ^{2,83}). We argue that the reasons for Sabatier's renaissance in the twenty-first century are twofold: the reaction, and his interest in operando spectroscopy. First, the increasing importance of hydrogenation reactions to convert organic molecules with renewably harvested hydrogen, and second, a revival of the importance of (operando) analysis techniques to better understand the functioning of (CO₂) hydrogenation catalysts. Both developments should provide society with novel or much-improved hydrogenation catalysts with tunable product selectivities.

Received: 1 October 2018; Accepted: 31 January 2019;

Published online: 11 March 2019

References

1. Senderens, J.-B. & Sabatier, P. Nouvelles synthèses du méthane. *Comptes Rendus Acad. Sci.* **82**, 514–516 (1902).
2. Sabatier, P. & Reid, E. E. *Catalysis in Organic Chemistry*. 2nd edn, (D. van Nostrand Company, New York, 1923).
3. Sabatier, P. & Senderens, J.-B. Hydrogénation directe des oxydes du carbone en présence de divers métaux divisés. *Comptes Rendus Acad. Sci.* **134**, 689–691 (1903).
4. Artz, J. et al. Sustainable conversion of carbon dioxide: an integrated review of catalysis and life cycle assessment. *Chem. Rev.* **118**, 434–504 (2018).
5. Rönsch, S. et al. Review on methanation — from fundamentals to current projects. *Fuel* **166**, 276–296 (2016).
6. Álvarez, A. et al. CO₂ activation over catalytic surfaces. *ChemPhysChem* **18**, 3135–3141 (2017).
7. Prieto, G. Carbon dioxide hydrogenation into higher hydrocarbons and oxygenates: thermodynamic and kinetic bounds and progress with heterogeneous and homogeneous catalysis. *ChemSusChem* **10**, 1056–1070 (2017).
8. Yang, H. et al. A review of catalytic hydrogenation of carbon dioxide into value-added hydrocarbons. *Catal. Sci. Technol.* **7**, 4580–4598 (2017).
9. Kattel, S., Liu, P. & Chen, J. G. Tuning selectivity of CO₂ hydrogenation reactions at the metal/oxide interface. *J. Am. Chem. Soc.* **139**, 9739–9754 (2017).
10. Rogelj, J. et al. Differences between carbon budget estimates unravelled. *Nat. Clim. Change* **6**, 245–252 (2016).
11. Hausfather, F. Analysis: how much 'carbon budget' is left to limit global warming to 1.5°C? *Carbon Brief* (9 April 2018); <https://www.carbonbrief.org/analysis-how-much-carbon-budget-is-left-to-limit-global-warming-to-1-5c>
12. Ricke, K. L. & Caldeira, K. Maximum warming occurs about one decade after a carbon dioxide emission. *Environ. Res. Lett.* **9**, 124002–124010 (2014).
13. Schlögl, R. The revolution continues: energiewende 2.0. *Angew. Chem. Int. Ed.* **54**, 4436–4439 (2015).
14. van Vuuren, D. P. et al. Alternative pathways to the 1.5 °C target reduce the need for negative emission technologies. *Nat. Clim. Change* **8**, 391–397 (2018).
15. *Shell Scenarios: Sky — Meeting the Goals of the Paris Agreement* (Shell, 2018).
16. Anderson, K. & Peters, G. The promise of negative emissions. *Science* **354**, 354–355 (2010).
17. Kramer, G. J. & Haigh, M. No quick switch to low-carbon energy. *Nature* **462**, 568–569 (2009).
18. Majumdar, A. & Deutch, J. M. Research opportunities for CO₂ utilization and negative emissions at the gigatonne-scale. *Joule* **2**, 805–809 (2018).
19. Bui, M. et al. Carbon capture and storage (CCS): the way forward. *Energy Environ. Sci.* **11**, 1062–1176 (2018).
20. *IPCC Carbon Dioxide Capture and Storage* (eds Metz, B., Davidson, O., de Coninck, H. C., Loos, M. & Meyer, L. A.) (Cambridge Univ. Press, 1975).
21. Kim, S. M. et al. Integrated CO₂ capture and conversion as an efficient process for fuels from greenhouse gases. *ACS Catal.* **8**, 2815–2823 (2018).
22. Stolaroff, J. K., Lowry, G. V. & Keith, D. W. Using CaO- and MgO-rich industrial waste streams for carbon sequestration. *Energy Convers. Manag.* **46**, 687–699 (2005).
23. House, K. Z. et al. Economic and energetic analysis of capturing CO₂ from ambient air. *Proc. Natl Acad. Sci. USA* **108**, 20428–20433 (2011).
24. Koytsoumpa, E. I., Bergins, C. & Kakaras, E. The CO₂ economy: review of CO₂ capture and reuse technologies. *J. Supercrit. Fluids* **132**, 3–16 (2018).
25. Keith, D. W., Holmes, G., St. Angelo, D. & Heidel, K. A Process for capturing CO₂ from the atmosphere. *Joule* **2**, 1573–1594 (2018).
26. Schlögl, R. E. Mobility and the energy transition. *Angew. Chem. Int. Ed.* **56**, 11019–11022 (2017).
27. Heide, D. et al. Seasonal optimal mix of wind and solar power in a future, highly renewable Europe. *Renew. Energy* **35**, 2483–2489 (2010).
28. Götz, M. et al. Renewable power-to-gas: a technological and economic review. *Renew. Energy* **85**, 1371–1390 (2016).
29. Gonzalez-Salazar, M. A., Kirsten, T. & Prchlik, L. Review of the operational flexibility and emissions of gas- and coal-fired power plants in a future with growing renewables. *Renew. Sustain. Energy Rev.* **82**, 1497–1513 (2018).
30. *Benchmarking of large scale hydrogen underground storage with competing options* (HyUnder, 2014).
31. Zhang, C. Hydrogen storage: improving reversibility. *Nat. Energy* **2**, 17064 (2017).
32. Aakko-Saksa, P. T., Cook, C., Kiviahio, J. & Repo, T. Liquid organic hydrogen carriers for transportation and storing of renewable energy — review and discussion. *J. Power Sources* **396**, 803–823 (2018).
33. Younas, M. et al. Recent advancements, fundamental challenges, and opportunities in catalytic methanation of CO₂. *Energy Fuels* **30**, 8815–8831 (2016).
34. Audi e-gas plant qualified to participate in balancing market to stabilize grid. *Green Car Congress* (15 July 2015); <https://www.greencarcongress.com/2015/07/20150715-egas.html>
35. The Sabatier system. NASA (12 May 2011); https://www.nasa.gov/mission_pages/station/research/news/sabatier.html
36. Muscatello, A. & Santiago-Maldonado, E. Mars in situ resource utilization technology evaluation. In *American 50th AIAA Aerospac Sciences Meeting* <https://doi.org/10.2514/6.2012-360> (AIAA, 2012).
37. Wang, W., Wang, S., Ma, X. & Gong, J. Recent advances in catalytic hydrogenation of carbon dioxide. *Chem. Soc. Rev.* **40**, 3703–3727 (2011).
38. Munnik, P., Velthoen, M. E. Z., de Jongh, P. E., De Jong, K. P. & Gommers, C. J. Nanoparticle growth in supported nickel catalysts during methanation reaction-larger is better. *Angew. Chem. Int. Ed.* **53**, 9493–9497 (2014).

39. Vogt, C. et al. Unravelling structure sensitivity in CO₂ hydrogenation over nickel. *Nat. Catal.* **1**, 127–134 (2018).
40. Heine, C., Lechner, B. A. J., Bluhm, H. & Salmeron, M. Recycling of CO₂: probing the chemical state of the Ni(111) surface during the methanation reaction with ambient-pressure X-ray photoelectron spectroscopy. *J. Am. Chem. Soc.* **138**, 13246–13252 (2016).
41. Silaghi, M., Comas-Vives, A. & Copéret, C. CO₂ activation on Ni/γ-Al₂O₃ catalysts by first-principles calculations: from ideal surfaces to supported nanoparticles. *ACS Catal.* **6**, 4501–4505 (2016).
42. Weatherbee, G. D. & Bartholomew, C. H. Hydrogenation of CO₂ on group VIII metals II. Kinetics and mechanism on nickel. *J. Catal.* **77**, 460–472 (1982).
43. Avanesian, T. et al. Quantitative and atomic-scale view of CO-induced Pt nanoparticle surface reconstruction at saturation coverage via DFT calculations coupled with in situ TEM and IR. *J. Am. Chem. Soc.* **139**, 4551–4558 (2017).
44. Studt, F. et al. Discovery of a Ni-Ga catalyst for carbon dioxide reduction to methanol. *Nat. Chem.* **6**, 320–324 (2014).
45. Wang, W. H., Himeda, Y., Muckerman, J. T., Manbeck, G. F. & Fujita, E. CO₂ hydrogenation to formate and methanol as an alternative to photo- and electrochemical CO₂ reduction. *Chem. Rev.* **115**, 12936–12973 (2015).
46. Kunkes, E. L., Studt, F., Abild-Pedersen, F., Schlögl, R. & Behrens, M. Hydrogenation of CO₂ to methanol and CO on Cu/ZnO/Al₂O₃: is there a common intermediate or not? *J. Catal.* **328**, 43–48 (2015).
47. Kitamura Bando, K., Sayama, K., Kusuma, H., Okabe, K. & Arakawa, H. In-situ FT-IR study on CO₂ hydrogenation over Cu catalysts supported on SiO₂, Al₂O₃, and TiO₂. *Appl. Catal. A* **165**, 391–409 (1997).
48. Andersson, M. P. et al. Structure sensitivity of the methanation reaction: H₂-induced CO dissociation on nickel surfaces. *J. Catal.* **255**, 6–19 (2008).
49. Abdel-Mageed, A. M., Eckle, S., Anfang, H. G. & Behm, R. J. Selective CO methanation in CO₂-rich H₂ atmospheres over a Ru/zeolite catalyst: the influence of catalyst calcination. *J. Catal.* **298**, 148–160 (2013).
50. Galletti, C., Specchia, S., Saracco, G. & Specchia, V. CO-selective methanation over Ru-γ-Al₂O₃ catalysts in H₂-rich gas for PEM FC applications. *Chem. Eng. Sci.* **65**, 590–596 (2010).
51. Iablokov, V. et al. Size-controlled model Co nanoparticle catalysts for CO₂ hydrogenation: synthesis, characterization, and catalytic reactions. *Nano Lett.* **12**, 3091–3096 (2012).
52. Sehested, J., Dahl, S., Jacobsen, J. & Rostrup-Nielsen, J. R. Methanation of CO over nickel: mechanism and kinetics at high H₂/CO ratios. *J. Phys. Chem. B* **109**, 2432–2438 (2005).
53. Zhu, W. et al. Active and selective conversion of CO₂ to CO on ultrathin Au nanowires. *J. Am. Chem. Soc.* **136**, 16132–16135 (2014).
54. Crampton, A. S. et al. Structure sensitivity in the non-scalable regime explored via catalysed ethylene hydrogenation on supported platinum nanoclusters. *Nat. Commun.* **7**, 10389 (2016).
55. Yang, H. B. et al. Atomically dispersed Ni(i) as the active site for electrochemical CO₂ reduction. *Nat. Energy* **3**, 140–147 (2018).
56. Van Helden, P., Ciobica, I. M. & Coetzer, R. L. J. The size-dependent site composition of FCC cobalt nanocrystals. *Catal. Today* **261**, 48–59 (2016).
57. Cargnello, M. et al. Control of metal nanocrystal size reveals metal-support interface role for ceria catalysts. *Science* **341**, 771–773 (2013).
58. Larmier, K. et al. CO₂-to-methanol hydrogenation on zirconia-supported copper nanoparticles: reaction intermediates and the role of the metal-support interface. *Angew. Chem. Int. Ed.* **56**, 2318–2323 (2017).
59. Kattel, S. et al. CO₂ hydrogenation over oxide-supported PtCo catalysts: the role of the oxide support in determining the product selectivity. *Angew. Chem. Int. Ed.* **55**, 7968–7973 (2016).
60. Li, S. et al. Tuning the selectivity of the catalytic CO₂ hydrogenation reaction by strong metal-support interaction. *Angew. Chem. Int. Ed.* **56**, 10761–10765 (2017).
61. Abate, S. et al. Catalytic performance of γ-Al₂O₃-ZrO₂-TiO₂-CeO₂ composite oxide supported Ni-based catalysts for CO₂ methanation. *Ind. Eng. Chem. Res.* **55**, 4451–4460 (2016).
62. Mebrahtu, C. et al. Hydrotalcite based Ni-Fe/(Mg, Al)_xO_y catalysts for CO₂ methanation-tailoring Fe content for improved CO dissociation, basicity, and particle size. *Catal. Sci. Technol.* **8**, 1016–1027 (2018).
63. Aldana, P. A. U. et al. Catalytic CO₂ valorization into CH₄ on Ni-based ceria-zirconia. Reaction mechanism by operando IR spectroscopy. *Catal. Today* **215**, 201–207 (2013).
64. Mutz, B. et al. Potential of an alumina-supported Ni₃Fe catalyst in the methanation of CO₂: impact of alloy formation on activity and stability. *ACS Catal.* **7**, 6802–6814 (2017).
65. Kustov, A. L. et al. CO methanation over supported bimetallic Ni-Fe catalysts: from computational studies towards catalyst optimization. *Appl. Catal. A* **320**, 98–104 (2007).
66. Sehested, J. et al. Discovery of technical methanation catalysts based on computational screening. *Top. Catal.* **45**, 9–13 (2007).
67. Liang, B. et al. Promoting role of potassium in the reverse water gas shift reaction on Pt/mullite catalyst. *Catal. Today* **281**, 319–326 (2017).
68. Cybulskis, V. J., Wang, J., Pazmiño, J. H., Ribeiro, F. H. & Delgass, W. N. Isotopic transient studies of sodium promotion of Pt/Al₂O₃ for the water-gas shift reaction. *J. Catal.* **339**, 163–172 (2016).
69. Zhou, M. & Liu, B. DFT investigation on the competition of the water-gas shift reaction versus methanation on clean and potassium-modified nickel(111) surfaces. *ChemCatChem* **7**, 3928–3935 (2015).
70. Ertl, G., Knözinger, H., Schüth, F. & Weitkamp, J. *Handbook of Heterogeneous Catalysis* 2nd edn. (Wiley-VCH, Weinheim, 2008).
71. Hou, C. T. *Handbook of Industrial Biocatalysis* (CRC Press, Boca Raton, 2005).
72. Hori, Y. in *Modern Aspects of Electrochemistry* Vol. 42 (eds Vayenas C. G., White R. E. & Gamboa-Aldeco M. E.) 89–189 (Springer, 2008).
73. Feng, J., Zeng, S., Feng, J., Dong, H. & Zhang, X. CO₂ electroreduction in ionic liquids: a review. *Chin. J. Chem.* **36**, 961–970 (2018).
74. Dinh, C.-T. et al. CO₂ electroreduction to ethylene via hydroxide-mediated copper catalysis at an abrupt interface. *Science* **360**, 783–787 (2018).
75. Xin, L. et al. Electricity storage in biofuels: selective electrocatalytic reduction of levulinic acid to valeric acid or γ-valerolactone. *ChemSusChem* **6**, 674–686 (2013).
76. Qiu, Y. et al. Integrated electrocatalytic processing of levulinic acid and formic acid to produce biofuel intermediate valeric acid. *Green Chem.* **16**, 1305–1315 (2014).
77. Kim, H. J., Lee, J., Green, S. K., Huber, G. W. & Kim, W. B. Selective glycerol oxidation by electrocatalytic dehydrogenation. *ChemSusChem* **7**, 1051–1054 (2014).
78. Kim, H. J. et al. Efficient electrooxidation of biomass-derived glycerol over a graphene-supported PtRu electrocatalyst. *Electrochem. Commun.* **13**, 890–893 (2011).
79. Hahn, C. et al. Engineering Cu surfaces for the electrocatalytic conversion of CO₂: controlling selectivity toward oxygenates and hydrocarbons. *Proc. Natl Acad. Sci. USA* **114**, 5918–5923 (2017).
80. Ni, Y. et al. Selective conversion of CO₂ and H₂ into aromatics. *Nat. Commun.* **9**, 3457 (2018).
81. Bai, S. et al. Highly active and selective hydrogenation of CO₂ to ethanol by ordered Pd-Cu nanoparticles. *J. Am. Chem. Soc.* **139**, 6827–6830 (2017).
82. Kowalczyk, Z. et al. Supported ruthenium catalysts for selective methanation of carbon oxides at very low CO₂/H₂ ratios. *Appl. Catal. A* **342**, 35–39 (2008).
83. Fecheté, I. Paul Sabatier — the father of the chemical theory of catalysis. *Comptes Rendus Chim.* **19**, 1374–1381 (2016).
84. *Guidance for Transporting Ammonia by Rail* (European Fertilizer Manufacturer Association, 2007).
85. Furler, P. et al. Solar kerosene from H₂O and CO₂. In *AIP Conf. Proc.* **1850**, 100006 (2017).
86. Martin, N. M. et al. Structure–function relationship during CO₂ methanation over Rh/Al₂O₃ and Rh/SiO₂ catalysts under atmospheric pressure conditions. *Catal. Sci. Technol.* **8**, 2686–2696 (2018).
87. Marwood, M., Doepper, R. & Renken, A. In-situ surface and gas phase analysis for kinetic studies under transient conditions — the catalytic hydrogenation of CO₂. *Appl. Catal. A* **151**, 223–246 (1997).

Acknowledgements

This work is supported by the Netherlands Organisation for Scientific Research (NWO) Gravitation program, Netherlands Center for Multiscale Catalytic Energy Conversion (MCEC), the Advanced Research Center Chemical Building Blocks Consortium (ARC CBBC) as well as from NWO in the form of a TA-CHIPP grant. H. Wiersma (Utrecht University) is acknowledged for his literature search and executing exploratory calculations.

Author contributions

C.V. and B.M.W. conceived the theme. C.V., M.M. and B.M.W. wrote the manuscript and designed the schemes and figures. G.J.K. contributed with insights and discussions. All authors contributed data and insights, discussed and edited the manuscript.

Competing interests

The authors declare no competing interests.

Additional information

Supplementary information is available for this paper at <https://doi.org/10.1038/s41929-019-0244-4>.

Reprints and permissions information is available at www.nature.com/reprints.

Correspondence should be addressed to B.M.W.

Publisher's note: Springer Nature remains neutral with regard to jurisdictional claims in published maps and institutional affiliations.

© Springer Nature Limited 2019